

BREAST CANCER AUGMENTATION USING AN INTEGRATED APPROACH OF REAL TIME SQUARE-ROI MARKER IDENTIFICATION AND VERIFICATION TECHNIQUES

Article history

Received

15 June 2015

Received in revised form

1 October 2015

Accepted

13 October 2015

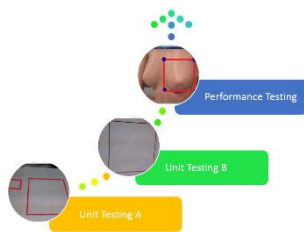
Rechard Lee*, Abdullah Bade

*Corresponding author

rl_mr@yahoo.com

Universiti Malaysia Sabah, Faculty of Science and Natural Resources, Department of Mathematics with Computer Graphics, Kota Kinabalu, Sabah, Malaysia

Graphical abstract



Abstract

The aim of this research is to develop a real-time Square-ROI marker identification and verification techniques by integrating the enhanced contour-corner approach. To enhance the conventional contour and corner approach, we proposed a smoothing and adaptive thresholding to the input stream captured via a webcam and then apply subpixel corner detection in order to obtain better and accurate corner points. For testing purposes, two sets of experiment have been set up to evaluate the proposed technique. The first experiment conducted by drawing a series of square-ROI on a paper. The subsequent experiment conducted with the use of a mannequin. Initially, during the experiment, the visual sensor (webcam) was positioned at 60 cm from the hand-drawn square-ROI in order to find the optimal distance needed by the proposed technique to define a marker. From the experiments, it reveals that the recognition technique in both testing setup was able to capture the real scene and convert the captured frame into a grey-scale image. Our evaluations on the series of square-ROI dataset shows that the proposed methods are robust to illumination changes and ROI's size, low in computation time, and greater in accuracy.

Keywords: Contour, Corner, Integrated, Marker, ROI

Abstrak

Tujuan kajian ini adalah untuk membangunkan teknik pengecaman dan pengesanan penanda segiempat-rantau sasaran (RS) masa nyata dengan mengintegrasikan pendekatan kontur-sudut yang telah dipertingkatkan. Untuk meningkatkan pendekatan kontur-sudut konvensional, pelicinan dan pengambangan penyesuaian diaplikasi ke atas aliran input yang diperolehi melalui kamera web dan kemudian subpiksel pengesanan sudut dilaksanakan untuk mendapatkan titik sudut yang lebih baik dan tepat. Dua set eksperimen telah direka untuk menilai teknik yang dicadangkan. Pertama, eksperimen dijalankan dengan melukis beberapa siri saiz segiempat-RS di atas kertas. Eksperimen seterusnya dijalankan dengan menggunakan model patung. Dalam setiap eksperimen, sensor visual (kamera web) diletakkan pada kedudukan 60 cm dari segiempat-RS untuk mencari jarak optimum yang diperlukan oleh teknik segiempat-RS dalam menentukan penanda. Daripada eksperimen yang dijalankan, teknik pengecaman segiempat-RS yang dibangunkan didapati lebih fleksibel dengan perubahan iluminasi dan saiz segiempat, masa pelaksanaan lebih rendah, dan lebih tepat.

Kata kunci: Kontur, Sudut, Integrasi, Penanda, Rantau sasaran

© 2016 Penerbit UTM Press. All rights reserved

1.0 INTRODUCTION

Comport [1] and Mellor [2] found that the use of computers in medicine has increased dramatically. This is due to the rapid development in computer processing power, display technology and needs among medical practitioner to properly plan a safe and friendly surgical operation [3]. Behringer [4], mentioned that Augmented Reality (AR) not only useful to visualize 3D medical data, but can be taken up as a tool to support surgical procedure. This will allow the surgeon to simultaneously examine the data and the patient.

In today medicine practices, there are two types of marker used by surgeons [5, 6, 7] either by using anatomical landmarks (non-invasive) or fiducial marker (invasive). Common fiducial markers used in surgeries are gold seeds or stainless steel screws that are implanted in and/or around a soft tissue tumor, or within the bony spine, to act as a landmark with millimeter precision. However, this method will require an additional surgery to attach or to insert the fiducial marker (see Figure 1) to the patient. It is not only time-consuming, but also invasive and might cause trauma to the patient. Patel [8] added, creation of a new foci of disease might be rare, but is a serious complication of fiducial marker placement. Due to its invasive implantation procedure [9] and the price of gold seeds are significantly higher [10], it is our aim to develop an alternative form of marker for cheaper, but efficient, robust and more patient-friendly through AR. Hence, innovations in the current insertion techniques of fiducial marker may reduce its risks, and at the same time enhancing comfort for the patient.

There are several situations where surgeons need to define Region-of-Interest (ROI). It can be drawn manually by hand or digitally by using a specific image processing technique. ROI is most commonly used for medical imaging as a subset of an image or as a contour defining a physical object that is of concern during a diagnosis. The ROI drawings can be used as two major functions [11]: (i) to examine the morphological properties of anatomic structure, and

(ii) to extract data for a specific structure. And, it also defines a specific shape (square or circle) which can be integrated with the AR technology as the fiducial marker. Owen [12] conclude that, an ideal fiducial marker should produce at least four points which are approximate a square. The straight edges of a square, allowing corners to be computed with sub-pixel accuracy. Four points not in the form of a square will decrease tracking accuracy due to poor resolution and orientation. Based on these findings, we believe that, ROI in the shape of a square will be an ideal marker for a surgeon in medical application.

Iris [13] considered the use of Computer Vision (CV) techniques as a starting point in detecting a fiducial marker or natural marker in order to solve the registration and tracking issues in an AR application. Edge detection, corner detection, blob detection, and optical flow are the current available technique that detects features.

Therefore, this paper aims to present a real-time pre-placed marker-less identification (RPMS) technique by integrating edge and corner approach to detect a square-ROI as the fundamental component in registering the virtual imagery with its real object without the needs to use the conventional fiducial marker. The main contributions of this paper can be summarized as follows:

- **Algorithms.** We propose robust, low computation time, and greater accuracy for both square and corner detection, respectively;

- **Experimental Evaluation.** Our evaluations on the series of square-ROI dataset shows that the proposed methods are robust, low in computation time, and greater in accuracy.

The rest of the paper is organized as follows; we outline the proposed marker recognition technique's framework in Section II. We investigate and evaluate the proposed algorithms in Section III. We conclude in Section IV.

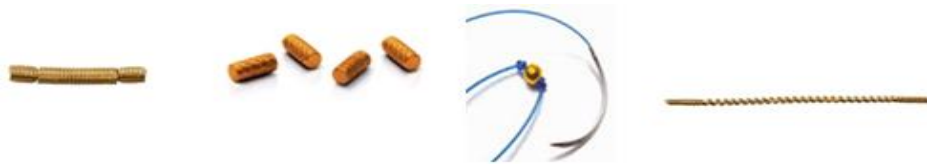


Figure 1 Example of breast marker use in medicine

2.0 LITERATURE

Several researchers, have made an effort to integrate the corner - contour approach with the perspective to define an edges as a square. But, until recently, the results showed that, some integrated technique are able to detect the square's corner, but fail to detect an edge point around the corners of the square.

For this reason, practical and feasible marker recognition technique using the advantages of both corner-contour approach with the manually hand-drawn ROI as an input which are efficient, accurate and robust is presented and shown in Figure 2. As can be seen, the proposed technique is the integration of two other techniques; i.e. square-ROI Contour and square-ROI corner.

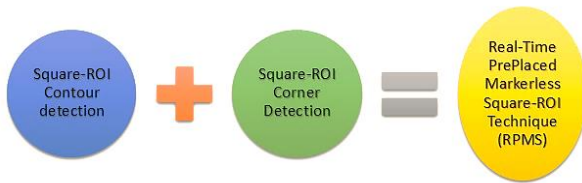


Figure 2 Integrated RPMS technique

To be a viable marker recognition technique, this algorithm is designed to have a minimal computational requirement and operates in two stages; i.e. square-ROI contour detection followed by square-ROI corner detection and tracking. Chapter four demonstrates how the improved square-ROI contour able to find the edges (in 0.16 ms) and define the detected edges as a square in order to extract the number of vertices. This is sufficient to be used as an initializer for the subsequent corner tracking technique described in chapter five. It is worth noting here that the success of the RPMS technique depends entirely on the success of the other two components. Thus, the ability of the proposed technique to efficiently and accurately define a marker at a minimal computation time rely on how fast the information (vertices and corners) can be produced at the early stage.

A. Improved Square-ROI Contour

To add the ability to detect and to define the square-ROI as a square, the traditional Canny's [14] operator is improved with adaptive thresholding and smoothing approach, then combine with the square contour detection method. Briefly, the improvement steps begins with smoothing in order to reduce the video stream noise followed by adaptive thresholding to create binary format and later the Canny's operator is used to find and extract the line edges from the binary format.

B. Enhanced square-ROI Corner

To enhance the ability of Shi-Tomasi [15] in detecting a desired corner point, our proposed technique combines Shi-Tomasi with subpixel and smoothing operation. As discussed in [15], the Shi-Tomasi directly determines the corners based on whether the minimum of two eigenvalues (λ_1, λ_2) is larger than a certain pre-defined threshold value and the subpixel operator is used to find an accurate location of a corner, based on the mathematical fact that the dot product of every vector from the centre to a point located within a neighborhood of an orthogonal vector is zero [16].

3.0 TESTING METHODOLOGY

The experiments are conducted according to the bottom-up testing approach as shown in Figure 3. The procedure begins with unit testing A and B, followed by the performance testing. These experiments are designed to investigate three main factors: (in terms of computation time, corner localization accuracy and its robustness)

1. The performance of square-ROI contour algorithm compared to the traditional Canny approach.
2. The performance of square-ROI corner algorithm compared to the traditional Shi-Tomasi approach.
3. The performance of the integrated RPMS technique compared to the ARToolkit.

These experiments use the Logitect web camera as the visual sensor to capture a real-time video from the real scene, a series of square-ROI's sizes ranging from 3x3 cm to 10x10 cm with 1.0 mm border line thickness, and a mannequin. The series of size were chosen based on the recommended marker size discussed in [12], and [17].

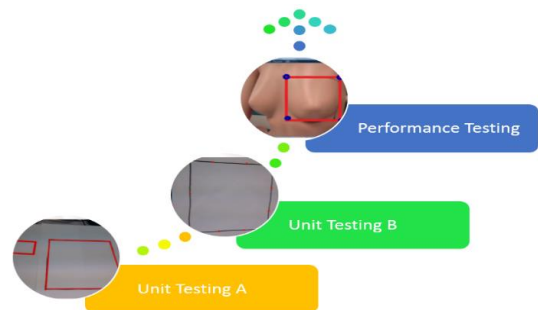


Figure 3 Experiments procedure

In the experiments, the visual sensor is initially positioned at 60 cm from the input (see Figure 4). This

will be the initial viewing distance for all the conducted test cases.

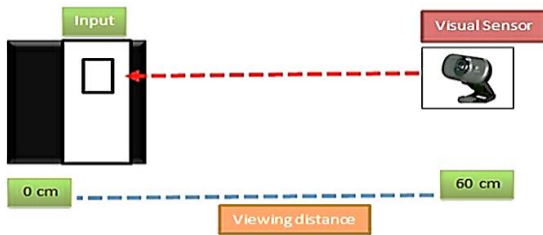


Figure 4 Camera viewing distance

3.0 RESULTS AND DISCUSSION

3.1 Unit Testing A-Square-ROI Contour Evaluation

Unit testing A consists of two experiments that were carried out to analyze the performance of square-ROI contour detection. First, the focus of these experiments lies on the testing of the Improved square-ROI contour compared to the Canny operator [14] and Sobel detector [18]. As shown in Figure 5, the improved operator has a better detection effect, compared with the image in (a) and (c). In (b), it is obviously has been improved. From the visual inspection of the images obtained, it can be seen that the Improved square-ROI contour is more efficient in identifying the edges clearly. The edge smoothly detected and almost no noise pixels detect on the input frame, hence, produces smooth and thin edges. Using traditional Canny and Sobel method, the edges detected are too messy and the data almost lost its important structure. The pixel is noisy and the edges are not smooth and thin.

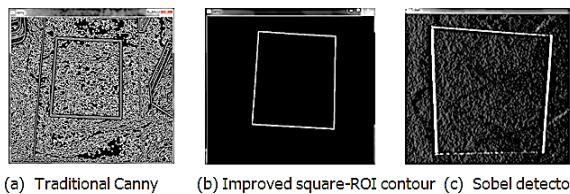


Figure 5 Experimental results-Edge detection

From Table 1, the proposed technique has gained 94.8% in speed (in ms) when compared with Canny operator and 98.4% when compared with Sobel detector. This indicates that the improved operator is more efficient and can enhance the hand-drawn square-ROI edges better than the other two tested approaches on edge detection. These results also solved the issues stated by [19], [20] and support the suggestion in [18], [21, 22, 23], where the use of adaptive edge-detection algorithm has improves the edge detection performance efficiency and speed.

Table 1 Average Time for edge detection

Operator	Canny detector	Sobel detector	Improved square-ROI contour
Average Time (ms)	6.08	20.9	0.16

In the second experiment, the testings are performed to determine the proposed technique's performance in identifying the detected edges as a square when the improved edge operator combined with the square contour. For each different ROI, the optimal viewing distance and the time required to identify a square, are recorded. At the same time, the robustness of the square-ROI contour will be assessed based on its consistency and accuracy in detecting the square in the given datasets.

Table 2 shows the results of Square-ROI contour's consistency and performance accuracy with eight different square-ROI's size. It is shown that the improved algorithm accurately identified the detected edges as a square, consistently from 7 to 10 cm for all given size. It should be noted that, the time-to-detect recoded from this experiment are the combination of edge detection and square contour identification. We have calculated that, for each ROI, an additional 13.45 to 18.89 ms are required to identify the detected edges as a square. Referring to Table 2, the best viewing distance and time-to-detect are obtained when the algorithm applies on 3 x 3 square-ROI size. It is the longest viewing distance recorded, and 13.76 to 16.39 ms required to define the square. Finally, Table 2 also shows that, by constructing different size of ROI the square-ROI contour technique is not only robust to illumination changes, but also to the variation of sizes.

Table 2 Square-ROI contour performance on series of ROI's sizes

Square-ROI size	Optimal Viewing Distance (cm)	Time to detect (ms)
3 x 3	7 - 29	13.76 - 16.39
4 x 4	7 - 24	13.7 - 16.52
5 x 5	7 - 14	13.62 - 18.31
6 x 6	7 - 17	14.05 - 16.32
7 x 7	7.5 - 15	13.46 - 19.05
8 x 8	7.5 - 15	13.51 - 16.8
9 x 9	8 - 14	13.61 - 16.86
10 x 10	10 - 17	13.74 - 14.07

Experimental results show that, the proposed technique efficiently detects and defines the desired hand-drawn square-ROI as a square within an acceptable execution time. It is also robust to illumination changes and accurately detects only the square-ROI.

3.2 Unit Testing B-Square-ROI Corner Evaluation

In this experiment, the testings are performed to determine the corner localization accuracy and computation efficiency of Enhanced square-ROI corner in extracting the four corner points from the detected edges. The experiments are repeated for eight different square-ROI's size, ranging from 3 x 3 cm to 10 x 10 cm with 1.0 mm border thickness, which is manually drawn by user. For each different square-ROI size, the experiments are tested for 49 cycles within the predefined visual distance in order to find the optimal viewing distance, execution time, and the average time required to find the four corners.

Figure 6 shows the results, in which eight different sizes for the algorithms are compared. The best viewing distance is obtained when the visual sensor is set at 23 cm from the square-ROI. This indication shows that the differences in size and visual distance have direct effects on the result. Significant improvements in corner detection for the proposed technique is recorded for both execution time and average time over the Shi-Tomasi [15] and Harris [24] method.

In short, the difference from the time construction show that, the Enhanced square-ROI has reduced the execution time by 0.17 ms (0.88%) and the average computation time by 0.14 ms (0.69%) when compared to Shi-Tomasi. However, when compared with Harris, the proposed technique produces no improvement in the execution time, but in overall the average execution time has reduced by 3.14 ms (12.9 %).

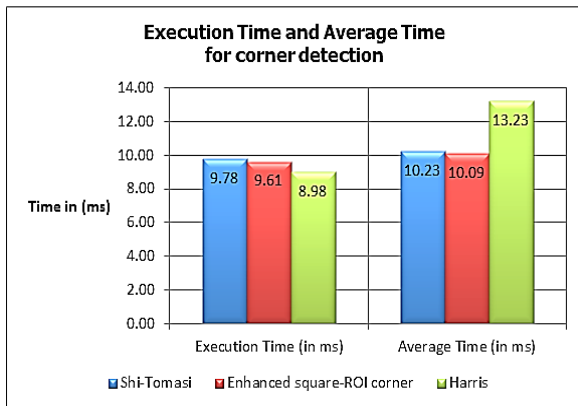


Figure 6 Execution Time and Average Time of Enhanced square-ROI corner, Shi-Tomasi, and Harris

These results solved the issues stated by [15] and support the suggestion in [25], [26], where the use of *subpixel corner-detection* algorithm has improved the corner detection performance efficiency and accuracy. Even though, the used of subpixel as discussed in [27] is said to be time consuming, in the experiments, our improved technique has shown that, when it is applied at a smaller scale of target

corner points, it effectively helps in improving the speed and the accuracy of the corner localization.

In Figure 7, it is clearly shown that from the visual inspection, the best precision results in corner localization are obtained when the algorithm applies subpixel accuracy (in (b)). Pay attention to the corner (red dot) found at the edge intersection. The corner detector in (b) has good localization compared to corner detector in (a).

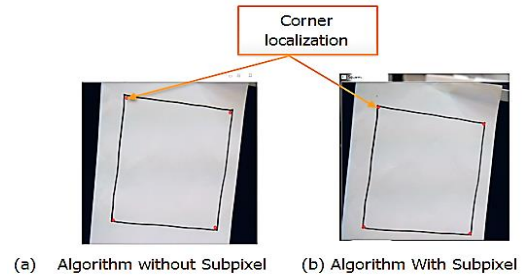


Figure 7 Corner localization

In the experiments, the performance of the square-ROI corner technique has improved even though the visual sensor need to be adjusted accordingly to get the four corners. Besides, with the proposed technique, the corner points are well localized.

3.3 Performance Testing –RPMS Evaluation

Performance testing consists of three experiments that were carried out to analyze the performance of RPMS technique. First, the focus lies in the RPMS performance accuracy in identifying the hand-drawn ROI on an A4 paper as a marker, followed by the used of a mannequin in the second experiment. In addition to that, our experiments also have the goal of determining how robust the RPMS approach is to variations in square-ROI sizes, in two different settings; i.e. an A4 paper and a mannequin.

Table 3 and Figure 8 show the results of the RPMS's consistency and accuracy performance with eight different square-ROI's size on A4 paper. It is shown that, the RPMS technique consistently identified all the given square-ROI as a marker in an average of 1.38 ms between 9 – 21 cm, with 0.9 ms for each execution. This indicates that the RPMS is more efficient than that of [28]. The best execution times are obtained when the RPMS technique applies on 6 x 6 cm square-ROI size, with 0.39 ms, followed by 5 x 5 cm (0.72 ms) and 10 x 10 cm (0.82 ms).

However, for the optimal viewing distance, mixed results have been recorded. It is found that for the size of 6 x 6 cm, the optimal viewing distance is from 7 – 23 cm, followed by 8 – 25 cm (7 x 7 cm) and 8 – 22 cm (8 x 8 cm). From here, the ROI setting with the best execution time and optimal viewing distance will be 6 x 6 cm and 10 x 10 cm.

Table 3 RPMS's experimental results on A4 paper

Square-ROI Size	Average (ms)	Time	Viewing Distance (cm)
3 x 3	2.20		8 – 20
4 x 4	1.21		8 – 16
5 x 5	0.72		9 – 18
6 x 6	0.39		7 - 23
7 x 7	1.35		8 - 25
8 x 8	1.73		8 – 22
9 x 9	2.60		10 – 20
10 x 10	0.82		11 – 23

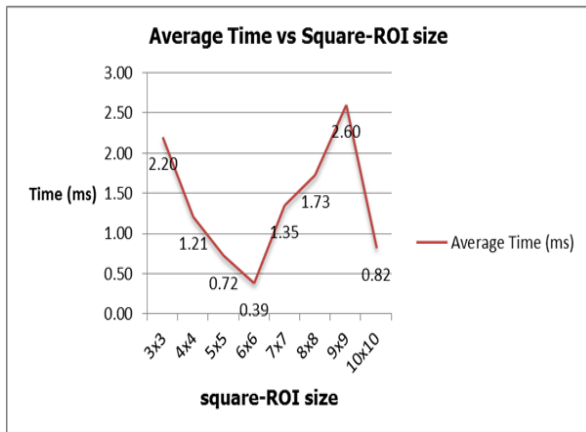


Figure 8 Average Time over Square-ROI's size

In most cases, the RPMS consistently identified a marker when used with the A4 paper. However, with the mannequin, there are situations where the RPMS fail to define a marker, even though it shows reasonable high percentage of true detection over false detection. There are two factors contributing to the 12.6% false detection percentage depicted in Figure 9, the size of the square-ROI and its visibility or occlusion problem.

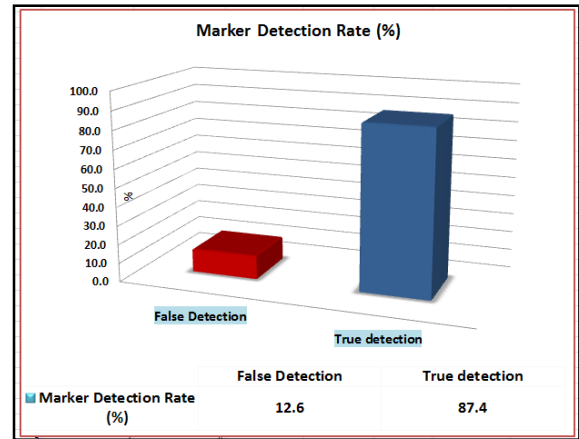


Figure 9 Marker detection rate - Mannequin

In the third experiment, the testings are performed to evaluate the performance of RPMS technique when compared with the ARToolkit in identifying a marker on A4 paper size. The testings are repeated 26 times independently with eight different sizes of ROI. There are two parameters tested in this experiment, i.e. execution time and detection accuracy. The recorded results are shown in Table 4. It is not surprising for the ARToolkit to be low in accuracy (11.5%), since it is specifically designed for pattern marker with ID. It is obvious that, when the detection accuracy is low, the time needed to define a marker is high. In other word, the lack of accuracy has a direct impact on the execution time.

Table 4 Experimental results – RPMS vs ARToolkit

Technique	Average Time (ms)	Accuracy (%)
RPMS	1.73	100
ARToolkit	9.73	11.5

It is shown in the experimental results that when the detection of square-ROI contour and square-ROI corner is improved, the RPMS technique is also improved. In other words, when the enhanced feature detection method minimizes the execution time and accurately extract the features needed at a consistent rate, expensive post-processing is thus avoided.

4.0 CONCLUSION

RPMS technique is a combination of the first two contributions mentioned above. The square-ROI contour edge detector is required to define the detected hand-drawn ROI as a square, whereas the square-ROI corner detector is needed to detect the four corners from the defined square-ROI. Both

components are equally important in order to recognize the hand-drawn square-ROI as a marker.

In conclusion, based on the obtained results, some of the findings can be concluded as follows:

- The integrated contour-corner approach is feasible and reliable in identifying the square-ROI as a marker.
- The proposed technique is more reliable and high in accuracy when compared with the ARToolkit in identifying the hand-drawn ROI as a marker.
- Viewing distance, visibility and the size of the hand-drawn square-ROI have a direct effect on the overall performance of the RPMS technique.
- With the advantages of both feature detectors, the RPMS is robust to ROI's size and illumination changes.

Acknowledgement

The author would like to thank the GRAVLAB research group for their advice and support. This research is supported by a grant (FRGS0295-SG-1/2011) from the Ministry of Education (MOE), Malaysia.

References

- [1] Comport, A. I., Marchand, E., and Chaumette, F. 2003. A Real-Time Tracker For Markerless Augmented Reality. In: The Second IEEE and ACM International Symposium on Mixed and Augmented Reality, Proceedings. *IEEE Comput. Soc.* 2006: 36-45.
- [2] Mellor, J. P. 1995. *Enhanced Reality Visualization in a Surgical Environment*.
- [3] Fischer, J., Neff, M., Freudenstein, D., and Bartz, D. 2004. Medical Augmented Reality based on Commercial Image Guided Surgery. In: *EGVE'04 Proceedings of the Tenth Eurographics Conference on Virtual Environments*. 83-86.
- [4] Behringer, R., Christian, J., Holzinger, A., and Wilkinson, S. 2007. Some Usability Issues of Augmented and Mixed Reality for e-Health Applications in the Medical Domain. In: Holzinger A, ed. *HCI and Usability for Medicine and Health Care*. Springer Berlin Heidelberg. 255-266.
- [5] Balachandran, R., Fritz, M. A., Dietrich M. S., Danilchenko, A., Mitchell, J. E., Oldfield, V. L., Lipscomb, W. W., Fitzpatrick, J. M., Neimat, J. S., Konrad, P. E., and Labadie, R. F. 2014. Clinical Testing Of An Alternate Method Of Inserting Bone-Implanted Fiducial Markers. *Int. Journal of Comp. Assisted Radiology and Surgery*.
- [6] Augdal, S. 2005. Surface-based Markerless Patient Registration.
- [7] Maintz, J. B. A., and Viergever, M. A. 1998. A Survey Of Medical Image Registration. *Med Image Anal.* 2(1): 1-36.
- [8] Patel, Z., Retrouvey, M., Vingan, H., and Williams, S. 2014. Radiology Case Reports Tumor Track Seeding: A New Complication of Fiducial Marker Insertion. 9.
- [9] Ying, H., Song, J., Ren, X., and Wang, W. 2008. Fingertip Detection and Tracking Using 2D and 3D. 1149-1152.
- [10] Coles, C. E., Harris, E. J., Donovan, E. M., Bliss, P., Evans, P. M., Fairfoul, J., Mackenzie, C., Rawlings, C., Syndikus, I., Twyman, N., Vasconcelos, J., Vowler, S.L., Wilkinson, J.S., Wilks, R., Wishart, G. C., and Yarnold, J. 2011. Evaluation of Implanted Gold Seeds For Breast Radiotherapy Planning And On Treatment Verification: A Feasibility Study On Behalf Of The IMPORT Trialists. *Radiotherapy and Oncology*. 100(2): 276-281.
- [11] Oakes, T. 2008. Brain Maker 3D Volume-of-Interest (VOD) Drawing And Analysis, [Online] From: http://brainimaging.waisman.wisc.edu/~oakes/spam/BrainMaker_Intro.html. [Accessed on 6 June 2014].
- [12] Owen, C. B., Middlin, P., and Xiao, F. 2002. What is the Best Fiducial? 1st IEEE International Workshop on Augmented Reality Toolkit. *IEEE*. 8.
- [13] Idris, M. Y. I., Arof, H., Tamil, E. M., Noor, N. M., and Razak, Z. 2009. Review of Feature Detection Techniques for Simultaneous Localization and Mapping and System on Chip Approach. *Inf Technol J.* 8(3): 250-262.
- [14] Canny, J. A. 1986. Computational Approach to Edge Detection. *IEEE Trans Pattern Anal Mach Intell.* PAMI-8(6): 679-698.
- [15] Shi, J., and Tomasi, C. 1994. Good Features To Track. In: *Proceedings of IEEE Conference on Computer Vision and Pattern Recognition CVPR-94*. IEEE Comput. Soc. Press. 593-600.
- [16] Bradski, G., and Kaehler, A. 2008. *Learning OpenCV*. O'Reilly Media.
- [17] Kato, H., Billingham, M., and Poupyrev, I. 2000. *ARToolKit User Manual, Version 2.33*. Washington D.C.
- [18] Bin, L., and Yeganeh, M. S. 2012. Comparison for Image Edge Detection Algorithms. *IOSR J Comput Eng.* 2(6): 1-4.
- [19] Maini, R., and Aggarwal, H. 2009. Study and Comparison of Various Image Edge Detection Techniques. *Int. Journal of Image Processing*. 3(1): 1-12.
- [20] Wang, B., and Fan, S. 2009. An Improved CANNY Edge Detection Algorithm. In: *2009 Second International Workshop on Computer Science and Engineering*. IEEE. 497-500.
- [21] Bansal, B., Saini, J. S., Bansal, V., and Kaur, G. 2012. Comparison of Various Edge Detection Techniques. *Journal of Information and Operation Management*. 3(1): 103-106.
- [22] Jansi, S., and Subashini, P. 2012. Optimized Adaptive Thresholding based Edge Detection Method for MRI Brain Images. *Int. Journal of Computer Application*. 51(20): 1-8.
- [23] Sonka, M., Hlavac, V., and Boyle, R. 2008. *Image Processing, Analysis and Machine Vision*. Internatio. THOMSON.
- [24] Harris, C., and Stephens, M. 1988. A Combined Corner and Edge Detector. In: *Proceedings of 4th Alvey Vision Conference*. 147-151.
- [25] Xingfang, Y., Yumei, H., and Yan, L. 2010. An Improved SUSAN Corner Detection Algorithm Based On Adaptive Threshold. In: *2010 2nd International Conference on Signal Processing Systems*. Ieee. V2-V613 - V2-V616.
- [26] Ye, Z., Pei, Y., and Shi, J. 2009. An Improved Algorithm for Harris Corner Detection. In: *2009 2nd International Congress on Image and Signal Processing*. Ieee. 1-4.
- [27] Baggio, D. L., Emami, S., Escrava, D. M., Levgen, K., Mahmood, N., Saragih, J. and Shikrot, R. 2012. *Mastering OpenCV with Practical Computer Vision Projects*. Packt Publishing Ltd.
- [28] Coleman, S., Kerr, D., and Scotney, B. 2007. Concurrent Edge and Corner Detection. In: *2007 ICIP IEEE International Conference on Image Processing*. Ieee. V - 273 - V - 276.